学位論文（要約）

# Studies on the role of Cep169, a centrosome protein, in primary cilium formation

（中心体タンパク質 Cep169 の一次繊毛形成制御機構の研究）

平成 29 年 12 月　博士（理学）申請

東京大学大学院理学系研究科

生物科学専攻

新冨　美雪

# Table of contents

## Abstract

The primary cilium is an immotile antenna-like organelle that arises from the mother centriole. Recent accumulating lines of evidence have shown that the primary cilium functions as a signal sensor on the surface of quiescent cells and that its dysfunction is tightly associated with a class of human diseases collectively called ciliopathies. Despite its biological and clinical importance, the mechanism by which the formation of primary cilia is repressed in proliferating cells remains elusive. Cep169 is a recently identified microtubule plus-end tracking and centrosome protein. Although the roles of Cep169 in microtubule dynamics and stability have been studied, its potential involvement in the regulation of primary cilia formation remains to be determined. In this thesis, using proteomic and cell biological approaches, I have comprehensively investigated the mechanism by which Cep169 regulates primary cilium formation.

The mass spectrometry-based analysis identified hundreds of novel Cep169-interacting proteins in human HeLa cells. Remarkably, they included several centrosome and cilium proteins. Many posttranslational modifications, such as cell cycle-dependent phosphorylation, methylation, and ubiquitination, were also identified. These results raised the possibility that Cep169 participates in primary cilium formation. Therefore, I attempted to gain further insight into the relationship between Cep169 and

the primary cilium. The siRNA-mediated depletion of Cep169 from proliferating human RPE1 cells induced untimely primary cilium formation. The resultant ciliated cells eventually entered a quiescent state. Cep169 depletion also caused a marked increase in the amounts of the TTBK2 kinase, which was previously implicated in ciliogenesis, consequently promoting the dissociation of Cep97 and CP110 from the mother centrioles. Remarkably, neither untimely ciliogenesis nor Cep97 dissociation was observed in cells simultaneously depleted of Cep169 and TTBK2. Taken together, these results strongly suggested that Cep169 plays a central role in the inhibition of untimely primary cilium formation in proliferating cells, by preventing the TTBK2-mediated dissociation of Cep97.

# 1. Introduction

## 1.1. Centrosome

### 1.1.1. The structure and function of the centrosome

The centrosome is an organelle that acts as the microtubule organizing center (MTOC) in proliferating cells. It is found in most animal cells except for oocytes, but not in plant cells (Bettencourt-Dias and Glover, 2007; Conduit et al., 2015; Dumont and Desai, 2012; Masoud et al., 2013). In the centrosome, a pair of cylindrical-shaped centrioles (*i.e.*, mother centriole and daughter centriole) is connected with linker fibers at their proximal ends (Sluder, 2005). Distal appendages and subdistal appendages are attached to the distal end of the mother centrioles, but not that of the daughter centrioles. The pericentriolar material (PCM) contains hundreds of proteins, and is an amorphous mass that surrounds the two centrioles (Alves-Cruzeiro et al., 2014; Andersen et al., 2003). The gamma-tubulin ring complexes (γ-TuRC) within the PCM nucleate the astral and spindle microtubules (Figure 1) (Zheng et al., 1995). The microtubule is a tubular cytoskeletal structure, with a protofilament consisting of a heterodimer of alpha-tubulin and beta-tubulin. The triplet microtubule is also a major structural element of centrioles (Paintrand et al., 1992). Although numerous proteins have been identified as centrosomal proteins and microtubule-associated proteins, the means by which these proteins contribute to the structures and functions of centrosomes are largely unknown.

### 1.1.2. The centrosome cycle

The centrosome is duplicated in S-phase by the formation of orthogonally arranged nascent centrioles, at the proximal ends of each pre-existing centriole (Nigg, 2007; Nigg and Stearns, 2011). During G2-phase, PCM components accumulate around centrioles, thereby resulting in centrosome maturation (Palazzo et al., 2000). Upon entry into mitosis, the two centrosomes split and act as the poles of the bipolar mitotic spindle, and then become separated into daughter cells at the end of mitosis (Heald et al., 1997). When cells cease proliferation and enter a quiescent state or G0-phase, the centrosome migrates to the cell cortex, where it converts into a basal body, and its distal end fuses with the plasma membrane. The basal body then emanates a primary cilium (Sanchez and Dynlacht, 2016). When the cells re-enter the cell cycle, the primary cilium is rapidly disassembled and the pair of centrioles is reorganized (Pugacheva et al., 2007).

## 1.2. Primary cilia

### 1.2.1. Primary cilium formation upon cell quiescence

The primary cilium is an antenna-like, immotile organelle that exclusively appears in quiescent cells (Singla and Reiter, 2006; Tucker et al., 1979). Upon mitogen deprivation, ciliary vesicles accumulate at the distal end of the mother centriole from the Golgi apparatus and cytoplasm, and then the resultant vesicles turn into the ciliary bud (Kobayashi et al., 2014; Lu et al., 2015; Schmidt et al., 2012). Subsequently, the distal end of the mother centriole is elongated and attached to the plasma membrane through the ciliary bud (Schmidt et al., 2009; Tang et al., 2009). At this point, the

elongated mother centriole is rearranged into a structure termed the basal body, and becomes extruded to the outside of the plasma membrane, consequently initiating primary cilium formation (Figure 3) (Tanos et al., 2013). As primary cilia are never found in proliferating cells, the successive events mentioned above are expected to be strictly suppressed by cell cycle regulators (Sanchez and Dynlacht, 2016).

### 1.2.2. The structure and function of the primary cilium

The primary cilium consists of the ciliary membrane, the axoneme, and the cargo protein complex (Figure 4A) (Ishikawa and Marshall, 2011). While the axoneme of a motile 9+2 cilium has two central microtubule singlets in addition to a ring of nine outer microtubule doublets (called a 9+2 axoneme), the axoneme of an "immotile" non-motile primary cilium is a 9+0 structure that lacks key elements involved in ciliary motility, including the central pair of microtubule singlets and their surrounding proteins essential for ciliary motility (Figure 4B) (Satir and Christensen, 2007 ; Satir et al., 2010). Rapid polymerization and stabilization of microtubules are facilitated by alpha-tubulin N-acetyltransferase (αTAT1) (Shida et al., 2010). Various membrane proteins embedded in the ciliary membrane, such as G protein-coupled receptors (GPCR), serve as receptors for extracellular signals (Hilgendorf et al., 2016). Microtubule motor proteins, such as kinesins and dyneins, form complexes with intraflagellar transport (IFT) and cargo proteins and move along the axonemes of primary cilia. IFT is composed of two large complexes, IFT A and IFT B. The outward (or anterograde) movement is powered by kinesin, while the inward (or retrograde)

movement is powered by dynein (Ishikawa and Marshall, 2011). Since these complexes act as signal transporters, the primary cilium can serve as a signal sensor (*e.g.*, GPCR signals, hedgehog signals, mechanical forces) (Satir et al., 2010). IFT-containing complexes are reportedly required for primary cilium maintenance, and ablation of the IFT protein causes primary cilia disassembly (Kim et al., 2011; Rosenbaum and Witman, 2002). Thus the primary cilium has numerous important cellular functions, as described above, and its absence or dysfunction causes many types of diseases (*e.g.*, polycystic kidney, pigmentary degeneration of the retina), which are collectively called ciliopathies (Fry et al., 2014; Kurkowiak et al., 2015; Nachury, 2014; Pazour et al., 2000).

### 1.2.3. The molecular mechanism of primary cilium formation

The assembly and disassembly of primary cilia depend on the balance between opposite directional regulations (Sanchez and Dynlacht, 2016). For example, some proteins are known to have a negative impact on ciliogenesis in proliferating cells, whereas others promote it upon cell quiescence. Most of these proteins exhibit centrosomal localization, and their functions are tightly controlled under certain conditions. Among them, it has been clearly demonstrated that Cep97 forms a complex with CP110 at the distal end of centrioles, and that their depletion results in untimely primary cilium formation in proliferating cells (Kobayashi et al., 2011; Spektor et al., 2007). Furthermore, the overexpression of CP110 or Cep97 in quiescent cells causes the disassembly of primary cilia (Spektor et al., 2007). Likewise, the kinesin-13 family

microtubule- depolymerizing kinesin Kif24 substantially contributes to the inhibition of the ciliogenesis program (Kobayashi et al., 2011), and the intermediate filament scaffold protein Tricoplein collaborates with the protein kinase Aurora A and suppresses ciliogenesis (Inoko et al., 2012). Untimely primary cilium formation by the depletion of Trichoplein induces cells to enter the quiescent state (Inoko et al., 2012). The Tau tubulin kinase 2 (TTBK2) has been identified as a protein that promotes primary cilium formation, through a genetic screen in mouse (Goetz et al., 2012; Houlden et al., 2007). Remarkably, TTBK2 promotes the removal of CP110 and Cep97 from the distal ends of the mother centrioles (Cajanek and Nigg, 2014; Oda et al., 2014). However, the mechanism by which the action of TTBK2 is coordinated in proliferating cells is poorly understood.

### 1.3. Cep169

Cep169 was originally identified as a binding partner of CDK5RAP2 (also known as Cep215, a human homologue of *Drosophila* Centrosomin) (Mori et al., 2015a), which regulates centrosomal maturation by the recruitment of a γ-TuRC onto centrosomes (Barr et al., 2010; Choi et al., 2010; Terada et al., 2003). The human Cep169 protein consists of 1,334 amino acids and includes proline-rich regions and predicted coiled-coil regions. Cep169 reportedly localizes at centrosomes and directly interacts with the Cnn motif 1 (CM1) of CDK5RAP2 (Mori et al., 2015a; Wang et al., 2010). In addition, Cep169 interacts with the microtubule plus end-tracking protein EB1 at the microtubule-plus end, through three EB1-binding motifs (SxIP) present in Cep169

(Honnappa et al., 2009; Mori et al., 2015a). The ablation of Cep169 function in mammalian cells caused rapid depolymerization of interphase microtubules (Mori et al., 2015a). Moreover, Cep169 overexpression leads to the formation of microtubule bundles, and induces microtubule aggregation via crosslinking of adjacent microtubules through its tubulin-binding domain (Mori et al., 2015c). The above findings suggested that Cep169 regulates microtubule stability and dynamics through cooperative interactions with CDK5RAP2 and EB1, although unlike CDK5RAP2, Cep169 is not required for the assembly of gamma-tubulin onto the centrosome (Choi et al., 2010). Moreover, Cep169 undergoes CDK1/cyclin B-mediated phosphorylation during the G2-M transition. Its association with centrosomes during interphase is diminished during mitosis following CDK1-dependent phosphorylation (Mori et al., 2015b). However, the functions of Cep169 at centrosomes are still elusive, as compared to our knowledge of its functions at the microtubule plus ends. Therefore, in this thesis, I focused on the function of Cep169 at centrosomes.

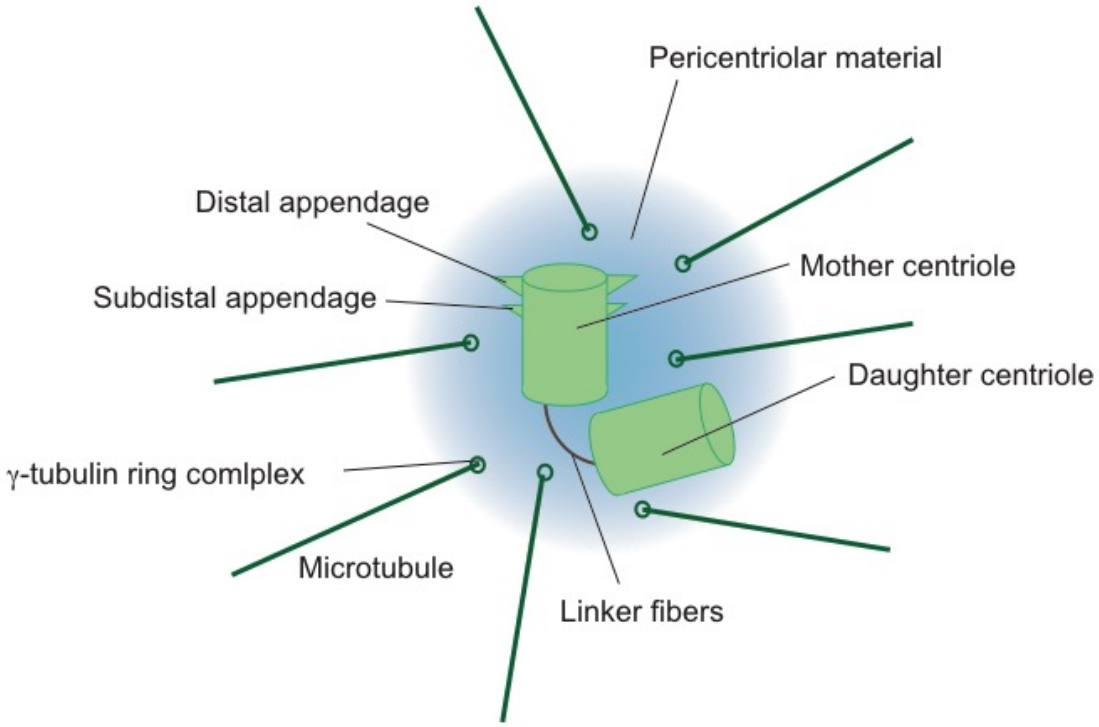


**Figure 1. The structure of the centrosome.**
The centrosome structure is depicted in the cartoon. See text for details.

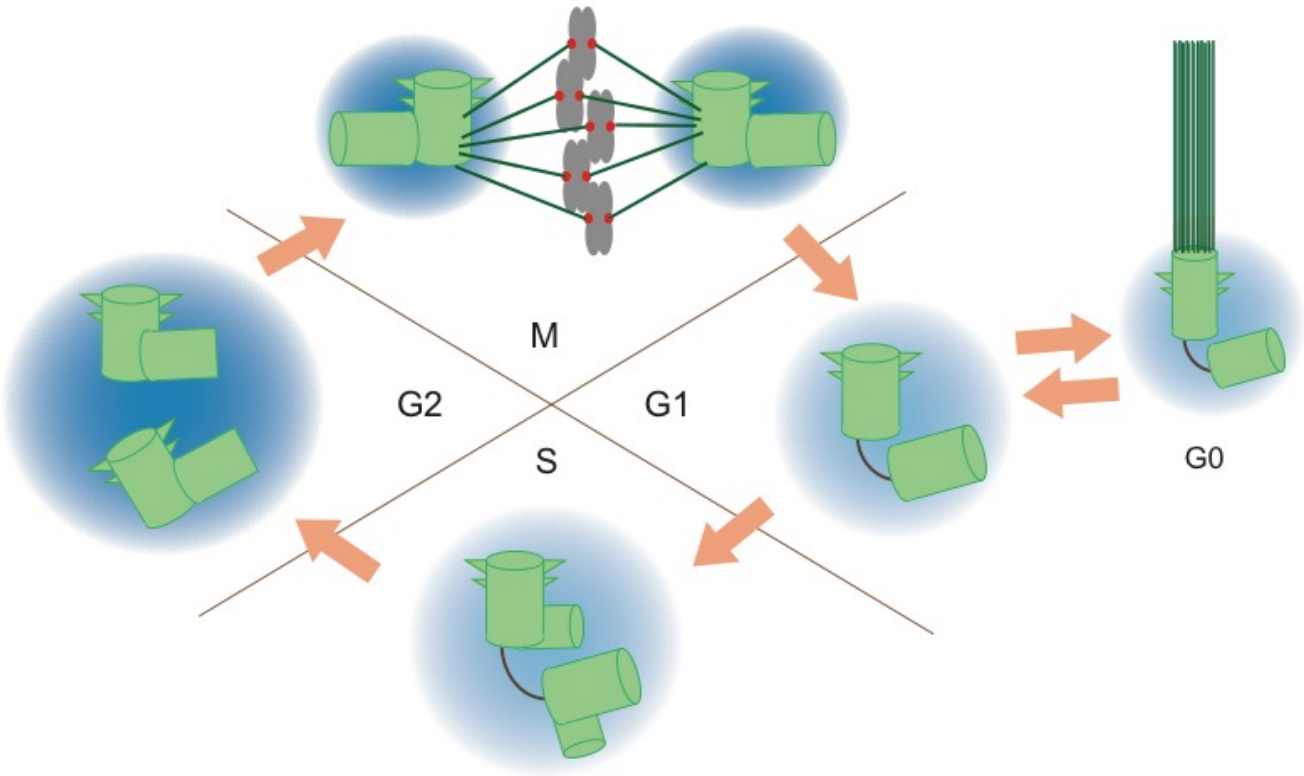


**Figure 2. The centrosome cycle.**
A schematic presentation of the centrosome cycle is shown. See text for details.

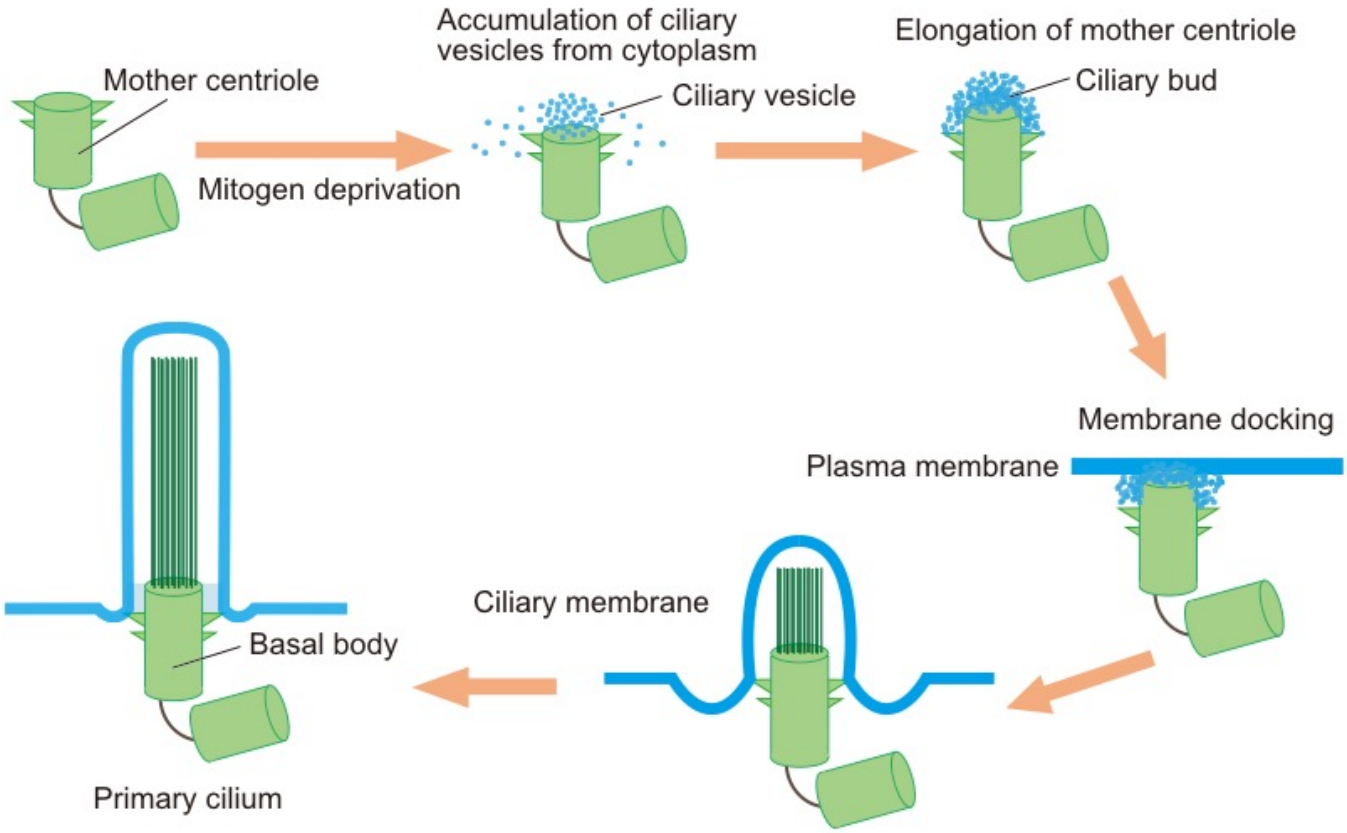


**Figure 3. Primary cilium formation upon cell quiescence.**
A schematic presentation of each step during primary cilium formation is depicted. See text for details.

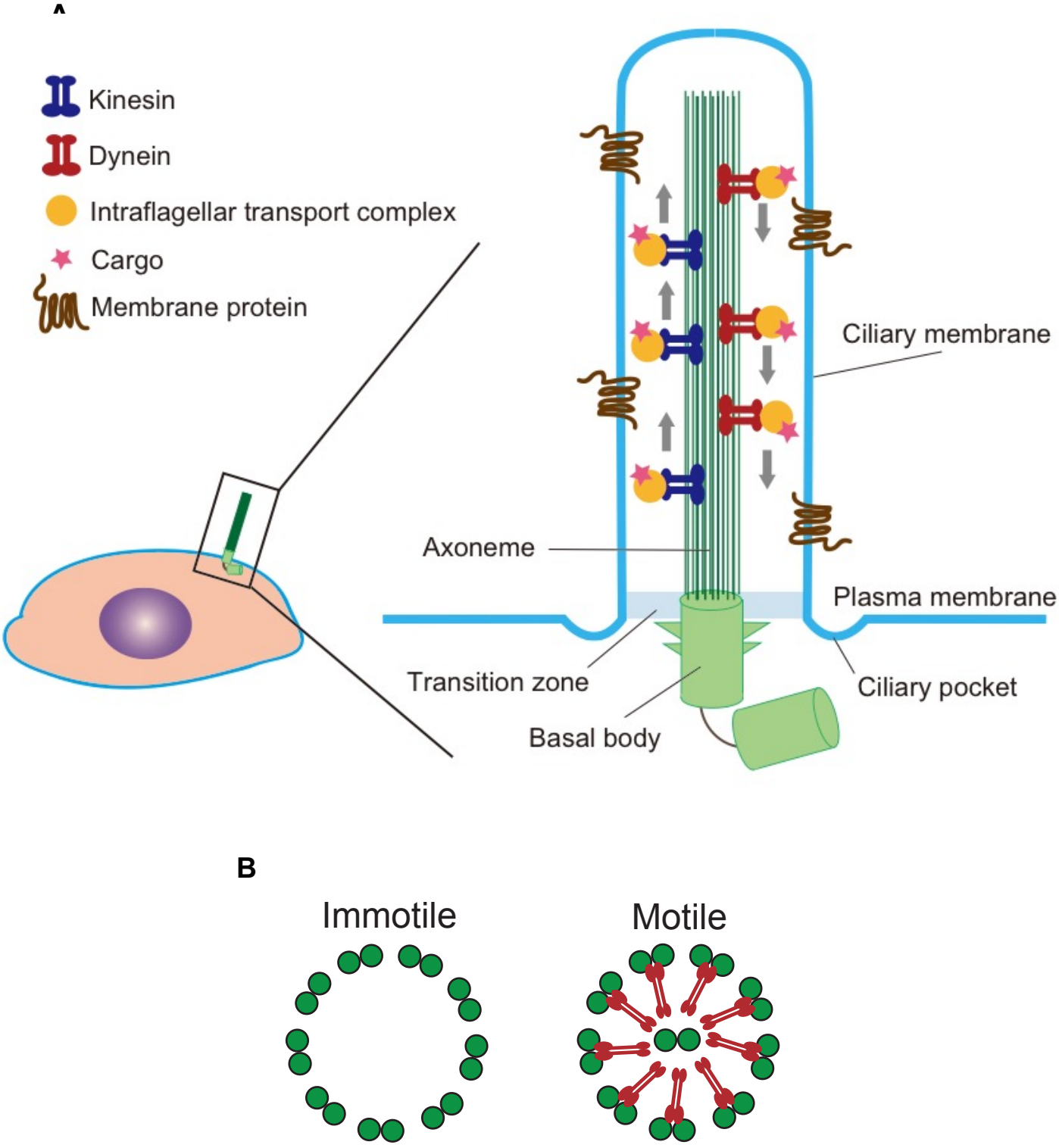


**Figure 4. The structure of the primary cilium.**

**(A)** The structure of the primary cilium is depicted in the cartoon. See text for details.

**(B)** The structure of the axoneme. See text for details.

## 2. Materials and methods

### 2.1. Cell culture and establishment of cell lines.

HeLa S3 cells (derived from human cervical cancer) and NIH3T3 cells (derived from mouse fibroblasts) were obtained from ATCC. hTERT-RPE1 cells (human TERT [telomere reverse transcriptase]-immortalized retinal pigment epithelial cells, referred to as RPE1) were provided by Dr. Tetsuo Kobayashi (Nara Institute of Science and Technology). The cells were maintained at 37°C in a 5% $CO_2$ atmosphere, in DMEM (Gibco) containing 10% fetal bovine serum (FBS) (Gibco) and penicillin-streptomycin (Wako).

To establish a HeLa S3 cell line in which the expression of FLAG-tagged Cep169 was conditionally induced by adding doxycycline, HeLa Flp-In™T-REx™ cells (Invitrogen) were transfected with the plasmid vector (FRT/TO-FLAG Cep169) (Mori et al., 2015a). To establish another RPE1 cell line that expresses doxycycline-inducible 3FLAG-HA-tagged Cep169, a recombinant retrovirus was produced by transfecting the virus packaging cell line 293T cells with a set of plasmid vectors, pMD2.G, psPAX2, and pInducer20-3FLAG-HA-Cep169, and then RPE1 cells were transfected with the resultant retrovirus.

### 2.2. Immunofluorescence microscopy

To prepare samples for immunofluorescence microscopy, cells were seeded and cultured on coverslips in DMEM-containing dishes. The cells attached to a coverslip were fixed with ice-cold methanol for 5 min, and then permeabilized with PBS containing 0.2%

Triton X-100 for 10 min. The coverslips were washed in PBS and immersed in PBS containing 3% BSA for 15 min, to prevent nonspecific antibody binding to the glass. This procedure was partly modified in the following cases. For probing acetylated-tubulin (a marker of primary cilia), cells attached to coverslips were immersed in cold PBS for 15 min to destabilize the cytoplasmic acetylated-tubulin, rather than the acetylated-tubulin within cilia, prior to fixation. For probing TTBK2, cells were fixed with 2% paraformaldehyde for 7 min prior to methanol fixation. Fixed cells were incubated with primary antibodies at 4°C overnight, and then washed in PBS three times. Incubation with secondary antibodies was performed at room temperature for 1 hr, and the coverslips were then washed five times in PBS. The DNA was counterstained with Hoechst 33342 (1:1000, Dojindo). The resultant coverslips were mounted on glass slides with 75% glycerol in PBS.

The fluorescent images shown in all figures, except for Figure 8E, were acquired with an FV3000 confocal microscope (Olympus), using Olympus 100x or 30x PlanApo objectives. In Figure 8E, an SD-OSR confocal microscope (Olympus), a high-speed SIM (structured illumination microscopy) system implemented on a spinning disc confocal microscope for super-resolution imaging was used. Z-sections were acquired at step sizes of 0.1-1 μm. Images were deconvolved and projected using the Cellsens software (Olympus). For the quantifications, all cells in the optic field were examined without any exception.

### 2.3. Immunoprecipitation

For the preparation of the cytoplasmic fraction, cells expressing FLAG-Cep169 were harvested, washed in PBS, and suspended in ice-cold cell lysis buffer (50 mM Tris-HCl, pH 7.5, 100 mM NaCl, 0.3% Triton X-100, and 10% glycerol), supplemented with the cOmplete™ protease inhibitor cocktail (Roche), the PhosSTOP™ phosphatase inhibitor cocktail (Roche), and 0.3 mM phenylmethyl sulfonyl fluoride. After an incubation in lysis buffer for 1 hr at 4°C, the suspension was centrifuged at 15,000 rpm, at 4°C, for 15 min to precipitate the insoluble materials. The recovered supernatant was used for immunoprecipitation, as the cytoplasmic fraction including centrosomes. For the preparation of anti-FLAG antibody-conjugated magnetic beads, the FLAG M2 antibody (Sigma, F1804) and Protein G-conjugated Dynabeads® (Thermo Fisher Scientific) were mixed and incubated for 1 hr, and then the antibody and beads were covalently crosslinked by adding dimethyl pimelimidate dihydrochloride (Sigma). For immunoprecipitation of FLAG-Cep169 and its associated proteins, the cytoplasmic fraction was incubated with antibody-conjugated magnetic beads at 4°C for 3 hr. The beads were washed in ice-cold lysis buffer three times, and in pre-elution buffer (50 mM Tris-HCl, pH 8.3, 500 mM NaCl, 1 mM EGTA) six times. The proteins were eluted by incubating the beads in elution buffer (50 mM Tris-HCl, pH 8.3, 1 mM EDTA, 0.3% SDS), with agitation, for 30 min. The eluted proteins were mixed with LDS sample buffer (Thermo Fischer Scientific) supplemented with 50 mM DTT and boiled. The samples were analyzed by SDS-PAGE and stained with a SilverQuest™ silver staining kit (Invitrogen).

## 2.4. Mass spectrometry

The immunoprecipitated proteins were prepared and separated by SDS-PAGE, as described in section 2.3, and the resultant silver-stained gel was sliced into 10 pieces. For in-gel digestion of proteins, each gel piece was incubated with Trypsin Gold Mass Spectrometry Grade (Promega) at 37°C for 16 hr. The digested peptides were dissolved in 0.1 % trifluoroacetic acid and subjected to liquid chromatography-tandem mass spectrometry (LC-MS/MS). The LC-MS/MS analysis was conducted with an LTQ-Orbitrap VELOS ETD mass spectrometer (Thermo Fisher Scientific), equipped with a nanoLC interface (AMR), a Paradigm MS2 nanoHPLC system (Michrom), and an HTC-PAL auto sampler (CTC Analytics). Each sample was loaded onto a trap column (0.3 mm ID x 5 mm, 5 μm, L-column; CERI) and a reverse phase C18 ESI column (0.1 mm ID x 150 mm, 3 μm, Zaplous α Pep-C18; AMR). The mass spectrometer was operated in the positive ionization mode, and the isolated charged ions were sequentially fragmented in the linear ion trap by collision-induced and electron-transfer dissociation. The protein annotation data were searched against the Uniprot protein sequence database of *Homo sapiens*, using the search program Proteome Discoverer™ 2.2 (Thermo Fisher Scientific), featuring the Sequest HT search algorithm for the identification of proteins and post translational modification sites. For quantification of phosphorylated peptides, I counted the PSMs detected using two types of precursor dissociation methods (CID and ETD).

### 2.5. siRNA-mediated depletion

For the siRNA-mediated depletion of various proteins in RPE1 cells, transfection was performed using Lipofectamine™ RNAi MAX (Invitrogen), according to the manufacturer's instructions. Two rounds of siRNA treatment were performed as depicted in Figure 9A, unless otherwise described. The sequences of the siRNAs are as follows:

Luciferase sense, 5′-CGUACGCGGAAUACUUCGATT-3′;

Luciferase antisense, 5′-UCGAAGUAUUCCGCGUACGTT-5′;

Cep169#1 sense, 5′-CUUGCCCAGGCCAACGAAAATT-3′;

Cep169#1 antisense, 5′-UUUUCGUUGGCCUGGGCAAGTG-3′;

Cep169#2 sense, 5′-GCAUGUACCAAGGUGCAGACACCTT-3′;

Cep169#2 antisense, 5′-AAGGUGUCUGCACCUUGGUACAUGCCA-3′;

TTBK2 sense, 5′-AGCAAGAAAUUGAUUCCAAAGAATG-3′;

TTBK2 antisense, 5′-CAUUCUUUGGAAUCAAUUUCUUGCUUG-3′;

Cep97 sense, 5′-GAUGAGAAGUGAAAUCAAUTT-3′;

Cep97 antisense, 5′-AUUGAUUUCACUUCUCAUCAT-3′;

IFT88 sense, 5′-CAAUCUAUGAUAUCGAGGAAUUGGA-3′;

IFT88 antisense, 5′-UCCAAUUCCUCGAUAUCAUAGAUUGGA-3′.

## 2.6. Antibodies

The primary antibodies used for western blotting and immunofluorescence were as follows: anti-FLAG (mouse clone M2, 1:1,000, Sigma, F1804); anti-Cep169 (rabbit, 1:100); anti-GAPDH (mouse clone GAPDH-71.1, 1:5,000, Sigma, G8795); anti-alpha-tubulin (mouse clone DM1A, 1:5,000, Sigma, T9026); anti-Ki67 (rabbit clone SP6, 1:500, Invitrogen); anti-gamma-tubulin (rabbit, 1:1,000, Sigma, T5192); anti-gamma-tubulin (mouse clone GTU-88, 1:1,000, Sigma, T5326); anti-acetylated tubulin (mouse clone 6-11B-1, 1:1,000, Sigma, T7451); anti-HA (rat clone 3F10, 1:1,000, Roche); anti-Cep97 (rabbit, 1:300, Sigma, HPA002980); anti-TTBK2 (rabbit, 1:500, Sigma, HPA018113); and anti-IFT88 (rabbit, 1:500, Proteintech, 13967-1-AP). The secondary antibodies used were as follows: anti-rabbit IgG, horseradish peroxidase (HRP)-conjugated (1:2,000; Santa Cruz Biotechnology, Inc.); anti-mouse IgG, HRP-conjugated (1:2,000, Santa Cruz Biotechnology, Inc.); anti-rat IgG, HRP-conjugated (1:2,000; Santa Cruz Biotechnology, Inc.); goat anti-mouse IgG, Alexa Fluor 568-conjugated (1:1,000, Invitrogen); goat anti-rabbit IgG, Alexa Fluor 568-conjugated (1:1,000, Invitrogen); goat anti-rabbit IgG, Alexa Fluor 488-conjugated (1:1,000, Invitrogen); goat anti-mouse IgG, Alexa Fluor 488-conjugated (1:1,000, Invitrogen); goat anti-rat IgG, Alexa Fluor 488-conjugated (1:1,000, Invitrogen); goat anti-rabbit IgG, Alexa Fluor 648-conjugated (1:1,000, Invitrogen); and goat anti-mouse IgG, Alexa Fluor 648-conjugated (1:1,000, Invitrogen).

### 2.7. Statistical analysis

The GraphPad Prism7 software (GraphPad Software) was used for all statistical analyses. For the analyses of three or more samples, one-way ANOVA with Bonferroni's multiple comparisons test was performed. For the analyses of two samples, the un-paired Student's t-test was performed.

### 2.8. Production of anti-Cep169 antibodies

To investigate endogenous Cep169, rabbit polyclonal antibodies were raised against recombinant human Cep169. To generate the hexahistidine (His6)-tagged antigen, the cDNA encoding amino acids 602-1334 of Cep169 was cloned into the pET28c plasmid vector. The His6-tagged antigen was produced in the *E. coli* BL21 (DE3) strain. The overexpressed protein was purified with Ni-NTA beads (QIAGEN) under denaturing conditions (containing 6 M guanidine-HCl), according to the manufacturer's instructions. The residual guanidine was removed by dialyzing the eluates against PBS overnight, with five buffer changes. Two rabbits were immunized four times, using 2 mg antigen protein for each immunization, followed by blood collection (conducted by Kiwa Laboratory Animals Co., Ltd.). For affinity purification of antibodies, antisera were absorbed to antigens immobilized on CNBr-Sepharose (GE Healthcare), and the bound antibodies were eluted in 100 mM glycine-HCl (pH 2.5). After elution, the eluates were neutralized with Tris-HCl, pH 8.8.

## 3. Proteomic analyses of Cep169

### 3.1. Results

#### *3.1.1. Cep169-interacting proteins are determined by mass spectrometry*

To identify Cep169-interacting proteins *in vivo*, a HeLa cell line expressing FLAG-Cep169 was established, and its lysates were processed for immunoprecipitation using an anti-FLAG antibody. The SDS-PAGE analysis of the precipitates showed that hundreds of different proteins interacted with Cep169 *in vivo*. The resultant gel was sliced into 10 pieces (from #1 to #10) (Figure 5A). After in-gel digestion with trypsin, the digested peptides were extracted from the gel pieces and subjected to liquid chromatography-tandem mass spectrometry (LC-MS/MS). LC-MS/MS analyses were performed by Dr. Lumi Negishi (assistant professor at the Institute of Molecular and Cellular Biosciences at The University of Tokyo). The MS/MS spectra were analyzed using the Proteome Discoverer™ software. The identified proteins with relatively high scores (> 30) are summarized in Figure 5B. The results showed that Cep169 interacted with microtubule-associated protein 1B (MAP1B), E3 ubiquitin ligases, adenomatous polyposis coli (APC), HSP70, and 14-3-3 proteins, in addition to the previously reported Cep169-interacting proteins, such as CDK5RAP2, tubulin, and actin (Mori et al., 2015a; Mori et al., 2015c). Furthermore, my analysis identified many kinds of Cep169-interacting proteins with lower scores, including centrosome components, cilium-regulating factors, microtubule-associated proteins (MAP), mitogen-activated kinases (MAPK), and E3 ubiquitin ligases (Fig. 5C). These data suggested that Cep169 has novel multiple functions in addition to the regulation of centrosomes, cilia, and

microtubules.

It was particularly interesting that Cep97 was identified as a novel Cep169-interating protein, because it had been implicated in primary cilia formation (Spektor et al., 2007). This physical interaction was further confirmed by the western blotting analysis of the precipitates associated with FLAG-Cep169 (Figure 5D). Therefore, I decided to perform functional analyses of Cep169 in the regulation of primary cilia formation. The details are described in the latter part of this thesis (Chapter 4).

### *3.1.2. Posttranslational modifications in Cep169 are identified by mass spectrometry*

Posttranslational modifications play a fundamental role in the regulation of cellular processes, and among them protein phosphorylation is one of the most important modifications for the regulation of protein function. Indeed, Mori et al. previously reported that mitotic Cdk1-mediated phosphorylation of Cep169 promotes its dissociation from the centrosome during mitosis (Mori et al., 2015b). To gain deeper insight into the *in vivo* functions of Cep169, I tried to determine the modification sites of Cep169 from extracts of asynchronously growing cells, by a proteomic analysis. Among a total of 27 phosphorylation sites identified (Figure 6A and B), S181, S440, S477, S571, S577, S735, S756, S767, S810, S813, S814, and S839 were annotated by more than five peptide spectrum matches (PSMs), indicating these 12 sites are strongly phosphorylated *in vivo* (Figure 6C). In particular, 14 sites were probably phosphorylated by cyclin-dependent kinases (collectively called CDKs), since they match the CDK consensus sequences, S*/T*-P and S*/T*-P-X-K/R (*, phosphorylated residue; X, any

amino acid) (Malumbres, 2014). The identified phosphorylated sites included seven novel CDK sites (S181, S498, S617, T659, S810, S814, and S839). Since these seven sites had not been identified in the previous analysis using mitotic cell extracts (Mori et al., 2015b), these residues were likely to be phosphorylated by CDK4 or CDK6 during G1 phase and by CDK2 during S and G2 phases. Furthermore, I identified three phosphorylation sites (S440, S577, and S767) that were identical to the MAPK consensus P-X-S*/T*-P (Shaul and Seger, 2007). In addition to the phosphorylation sites, four methylation sites, R163, R848, R886, and R1254, and four ubiquitination sites, K433, K683, K774, and K796, were identified (Figure 6A and B).

### 3.2. Discussion

It has been demonstrated that Cep169 regulates microtubule dynamics and stabilization with CDK5RAP2 (Mori et al., 2015a). Cep169 has also been shown to interact with EB1, a member of the microtubule plus-end-tracking proteins (+TIPs), through its EB1-binding motifs (S-X-I-P) and to localize at microtubule plus-ends. The depletion of Cep169 induces microtubule depolymerization and its overproduction bundles microtubules in the cytoplasm, leading to the formation of a solid microtubule structure by cross-linking adjacent microtubules as a homodimer (Mori et al., 2015c). However, we are still largely ignorant of how Cep169 contributes to microtubule stabilization with EB1. In this study, I identified several MAPs, including MAP1B (which is highly expressed in developing neurons) (Black et al., 1994), MAP7, and the microtubule-associated tumor suppressor 1 (also known as MTUS1), as binding partners with

Cep169. MAP1B interacts directly with the +TIPs EB1/3 and regulates microtubule dynamics by sequestering EB1/3 from the microtubule plus-end (Barr et al., 2010). Interestingly, MAP1B controls EB1/3 localization, mobility, and microtubule dynamics in extending neurites/axons and growth cones (Tortosa et al., 2013). It is therefore possible that Cep169 regulates microtubule dynamics and stability with MAP1B, to control EB1/3 localization at the microtubule plus-ends during neurogenesis.

The numerous Cep169-interacting factors that I have identified include several centrosome components: PCM1, CDK5RAP2, Cep295, Cep170, Cep131, Cep55, and SSX2IP, and cilium assembly-related proteins: Cep97, WDR8, BBS7, IFT140, and IFTM3. Among them, I confirmed that Cep169 interacts with Cep97, which prevents cilia formation with CP110 by capping mother centrioles (Kobayashi et al., 2011; Spektor et al., 2007). These data suggest that Cep169 might regulate ciliogenesis with these cilium proteins. This point is further addressed in this thesis (see Chapter 4).

Mori et al. reported that Cep169 dissociates from the centrosome during mitosis through CDK1-dependent phosphorylation (Mori et al., 2015b). Treatment of mitotic cells with Purvalanol A, a CDK inhibitor, strongly inhibits the dissociation of Cep169 from centrosomes. Indeed, mass spectrometry analyses previously identified seven CDK consensus sites phosphorylated in mitotic cells. Our current study revealed that seven additional CDK consensus sites were phosphorylated in asynchronous cells. It is most likely that these sites are phosphorylated by not only the mitotic CDK (*i.e.*, CDK1) but also the interphase CDKs (CDK4, CDK6, and CDK2). These results suggest

that the functions of Cep169 might be controlled by multiple layers of regulation, by various combinations of cyclins and CDKs throughout the cell cycle.

In addition to the phosphorylation modification, four ubiquitination sites in Cep169 were determined. Interestingly, I also found several E3 ligase complex subunits (TRAF7, TRIM21/37, ZNF598, MYLIP, RNF41, RNF135, Cullin-3, Cullin-4A/B, DDB1, and DCAF6) in the immunoprecipitates of Cep169. Thus, Cep169 might be targeted for degradation in a ubiquitin/proteasome-dependent manner. Although the current study also identified four arginine residues that could be methylated, their importance remains elusive at this point.

In summary, my proteomic analyses using extracts from an asynchronous culture of HeLa cells identified numerous proteins interacting with Cep169 and its *in vivo* modification sites. Although the knowledge about their physiological roles is still limited, future pursuits of my current observations will help to comprehensively clarify the divergent roles of Cep169 in centrosome assembly, microtubule dynamics, ciliogenesis, and cell division.

**A**

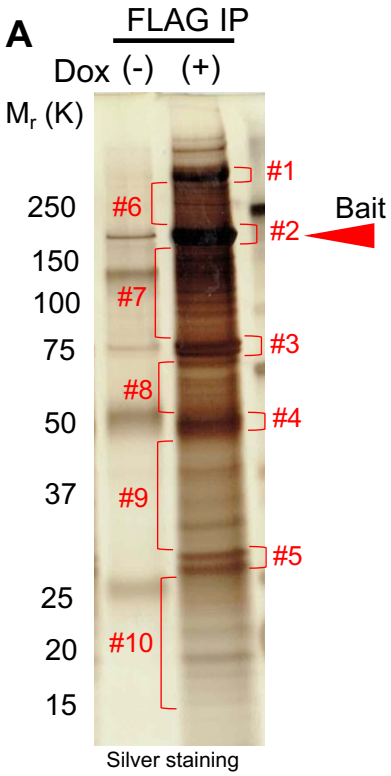


**B**

#1

| Description | Coverage | Score | # peptides |
|---|---|---|---|
| MAP1B | 46.15 | 485.97 | 94 |
| UBR5 | 20.11 | 139.78 | 46 |
| APC | 18.66 | 117.9 | 42 |
| FLNA | 13.71 | 78.43 | 28 |
| DSP | 6.58 | 34.84 | 17 |

#2

| Description | Coverage | Score | # peptides |
|---|---|---|---|
| Cep169 | 62.48 | 987.29 | 74 |
| SPAG5 | 22.72 | 64.50 | 17 |
| CLTC | 12.69 | 61.30 | 16 |
| CLUH | 14.90 | 50.29 | 18 |
| ANKRD50 | 10.57 | 47.16 | 11 |

#3

| Description | Coverage | Score | # peptides |
|---|---|---|---|
| HSPA1B | 71.50 | 470.12 | 44 |
| HNRNPM | 50.00 | 168.60 | 37 |
| DDX3X | 25.65 | 57.41 | 17 |
| DDX5 | 31.76 | 60.48 | 20 |
| DDX17 | 27.95 | 58.52 | 19 |
| PABPC1 | 29.09 | 57.42 | 16 |
| DDX3X | 25.65 | 57.41 | 17 |
| HAUS3 | 18.74 | 31.96 | 9 |

#4

| Description | Coverage | Score | # peptides |
|---|---|---|---|
| TUBB | 73.87 | 313.82 | 25 |
| TUBA | 59.42 | 227.78 | 21 |
| KRT18 | 58.14 | 141.71 | 28 |
| RUVBL2 | 53.56 | 76.75 | 22 |
| CTBP2 | 30.02 | 66.78 | 14 |
| PRKAR2A | 35.89 | 52.74 | 11 |
| EEF1A1 | 33.12 | 46.46 | 12 |
| TNIP2 | 30.07 | 35.33 | 14 |

#5

| Description | Coverage | Score | # peptides |
|---|---|---|---|
| YWHAE | 69.02 | 159.06 | 18 |
| YWHAQ | 55.10 | 128.05 | 15 |
| YWHAZ | 60.00 | 85.77 | 14 |
| YWHAG | 61.13 | 81.84 | 14 |
| YWHAH | 50.00 | 68.90 | 12 |
| RPS3 | 59.67 | 30.12 | 12 |
| SFN | 30.65 | 32.81 | 8 |

#9

| Description | Coverage | Score | # peptides |
|---|---|---|---|
| HNRPF | 26.51 | 49.44 | 7 |
| EMD | 49.61 | 47.43 | 12 |
| RPLP0 | 49.53 | 45.75 | 13 |
| ACTC | 28.12 | 41.94 | 10 |
| ANXA2 | 39.53 | 40.38 | 11 |
| HAUS4 | 39.39 | 36.07 | 14 |
| EIF4A1 | 27.09 | 33.17 | 10 |

#6

| Description | Coverage | Score | # peptides |
|---|---|---|---|
| CAD | 34.47 | 211.69 | 56 |
| MYO10 | 30.06 | 204.70 | 55 |
| USP9X | 27.20 | 198.27 | 62 |
| PLEC | 9.31 | 94.39 | 38 |
| USP9Y | 12.95 | 92.07 | 34 |
| SEC16A | 17.56 | 82.24 | 29 |
| RICTOR | 19.20 | 66.50 | 28 |
| PCM1 | 10.82 | 52.88 | 21 |
| SNRNP200 | 8.52 | 42.04 | 14 |

#7

| Description | Coverage | Score | # peptides |
|---|---|---|---|
| CEP169 | 42.71 | 296.05 | 49 |
| DDB1 | 45.53 | 172.37 | 47 |
| HSP90AA1 | 39.48 | 85.19 | 27 |
| CTNNA1 | 33.55 | 69.42 | 23 |
| DCAF6 | 27.56 | 56.64 | 20 |
| CUL4A | 31.88 | 46.13 | 21 |
| PFKP | 22.45 | 44.67 | 13 |
| HSPH1 | 25.52 | 42.93 | 17 |
| FAM83B | 19.09 | 42.50 | 14 |
| NDUFS1 | 28.75 | 41.47 | 14 |
| NUP155 | 10.42 | 41.45 | 11 |
| MATR3 | 18.32 | 41.27 | 13 |
| BAG3 | 27.65 | 40.88 | 14 |
| CTNNB1 | 24.07 | 37.67 | 16 |
| JUP | 19.60 | 32.46 | 13 |

#8

| Description | Coverage | Score | # peptides |
|---|---|---|---|
| HEL113 | 58.37 | 101.05 | 27 |
| HSPD1 | 43.98 | 63.70 | 18 |
| STK38 | 44.30 | 80.61 | 19 |
| HNRPK | 40.73 | 65.22 | 16 |
| TRAF7 | 41.64 | 59.58 | 21 |
| FBXW11 | 40.04 | 58.60 | 21 |
| TRIM7 | 34.25 | 54.94 | 15 |
| DNAJC7 | 38.66 | 54.14 | 19 |
| TRIM27 | 32.16 | 49.67 | 12 |
| PHGDH | 26.08 | 39.84 | 12 |
| SQSTM1 | 34.55 | 39.44 | 10 |
| BTRC | 21.86 | 37.43 | 13 |
| TRIM21 | 22.95 | 36.81 | 9 |
| PPP2R1A | 30.05 | 36.78 | 16 |
| CCT4 | 29.50 | 33.52 | 13 |

#10

| Description | Coverage | Score | # peptides |
|---|---|---|---|
| PDCD6 | 51.31 | 37.93 | 7 |

**C**

| Centrosome | MAP | Ubiquitin |
|---|---|---|
| PCM1 | MAP1B | UBR5 |
| CDK5RAP2 | MAP7 | CUL3 |
| Cep295 | MAP4 | CUL4A/B |
| Cep170 | MTUS1 | DDB1 |
| Cep131 | MAPK | DCAF6 |
| Cep55 | MAPK1 | TRAF7 |
| SSX2IP | MAP3K12 | TRIM21/37 |
| Cilium | MAP3K4 | ZNF598 |
| Cep97 | MAP3K6 | MYLIP |
| WDR8 | MAP4K4 | RNF41/135 |
| BBS7 | | |
| IFT140 | | |
| IFTM3 | | |

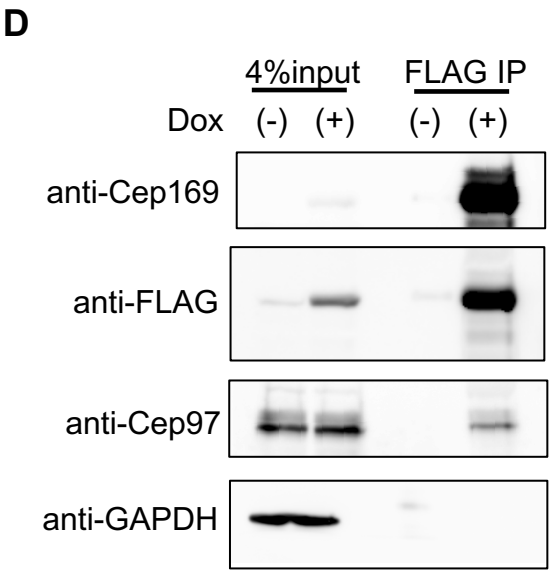


**Figure 5. Cep169-interacting proteins are determined by mass spectrometry.**
**(A)** A lysate prepared from HeLa S3 cells expressing FLAG-Cep169 was subjected to immunoprecipitation, using an anti-FLAG antibody (+ Dox). The precipitate was separated by SDS-PAGE and silver-stained. As a negative control, cells in which FLAG-Cep169 expression had not been induced (- Dox), was analyzed in parallel. The gel was sliced into 10 pieces (indicated by brackets) and processed for mass spectrometry. The arrowhead indicates the band corresponding to FLAG-Cep169.
**(B)** Cep169 interacting proteins were identified by analyzing tandem mass spectra using the Proteome Discover™ program. A summary of the identified proteins is shown. Proteins identified with low probability (scores lower than 30) and contaminants (*e.g.*, keratin and trypsin) are not listed.
**(C)** The identified Cep169-interacting proteins (including scores were lower than 30) were categorized. They include centrosomal components (centrosome), cilia-associated factors (cilium), microtubule-associated proteins (MAP), mitogen-activated protein kinase (MAPK), and subunits of E3 ubiquitin ligases (ubiquitin).
**(D)** Lysates prepared from control (- Dox) cells and cells expressing FLAG-Cep169 (+ Dox) were immnoprecipitated with an anti-FLAG antibody. The precipitates, along with aliquots of the lysates (input), were analyzed by western blotting using the indicated antibodies.

**A**

```
1-100       MSEAMDQPAG GPGNPRPGEG DDGSMEPGTC QELLHRLREL EAENSALAQA NENQRETYER CLDEVANHVV QALLNQKDLR EECIKLKKRV FDLERQNQML
101-200     SALFQQKLQL TTGSLPQIPL TPLQPPSEPP ASPSLSSTEG PAAPLPLGHC AGQREVCWEQ QLRPGGPGPP AAPPPALDAL SPFLRKKAQI LEVLRALEET
201-300     DPLLLCSPAT PWRPPGQGPG SPEPINGELC GPPQPEPSPW APCLLLGPGN LGGLLHWERL LGGLGGEEDT GRPWGPSRGP PQAQGTSSGP NCAPGSSSSS
301-400     SSDEAGDPNE APSPDTLLGA LARRQLNLGQ LLEDTESYLQ AFLAGAAGPL NGDHPGPGQS SSPDQAPPQL SKSKGLPKSA WGGGTPEAHR PGFGATSEGQ
401-500     GPLPFLSMFM GAGDAPLGSR PGHPHSSSQV KSKLQIGPPS PGEAQGPLLP SPARGLKFLK LPPTSEKSPS PGGPQLSPQL PRNSRIPCRN SGSDGSPSPL
501-600     LARRGLGGGE LSPEGAQGLP TSPSPCYTTP DSTQLRPPQS ALSTTLSPGP VVSPCYENIL DLSRSTFRGP SPEPPPSPLQ VPTYPQLTLE VPQAPEVLRS
601-700     PGVPPSPCLP ESYPYGSPQE KSLDKAGSES PHPGRRTPGN SSKKPSQGSG RRPGDPGSTP LRDRLAALGK LKTGPEGALG SEKNGVPARP GTEKTRGPGK
701-800     SGESAGDMVP SIHRPLEQLE AKGGIRGAVA LGTNSLKQQE PGLMGDPGAR VYSSHSMGAR VDLEPVSPRS CLTKVELAKS RLAGALCPQV PRTPAKVPTS
801-900     APSLGKPNKS PHSSPTKLPS KSPTKVVPRP GAPLVTKESP KPDKGKGPPW ADCGSTTAQS TPLVPGPTDP SQGPEGLAPH SAIEEKVMKG IEENVLRLQG
901-1000    QERAPGAEVK HRNTSSIASW FGLKKSKLPA LNRRTEATKN KEGAGGGSPL RREVKMEARK LEAESLNISK LMAKAEDLRR ALEEEKAYLS SRARPRPGGP
1001-1100   APGPNTGLGQ VQGQLAGMYQ GADTFMQQLL NRVDGKELPS KSWREPKPEY GDFQPVSSDP KSPWPACGPR NGLVGPLQGC GKPPGKPSSE PGRREEMPSE
1101-1200   DSLAEPVPTS HFTACGSLTR TLDSGIGTFP PPDHGSSGTP SKNLPKTKPP RLDPPPGVPP ARPPPLTKVP RRAHTLEREV PGIEELLVSG RHPSMPAFPA
1201-1300   LLPAAPGHRG HETCPDDPCE DPGPTPPVQL AKNWTFPNTR AAGSSSDPLM CPPRQLEGLP RTPMALPVDR KRSQEPSRPS PTPQGPPFGG SRTPSTSDMA
1301-1334   EEGRVASGGP PGLETSESLS DSLYDSLSSC GSQG
```

**B**

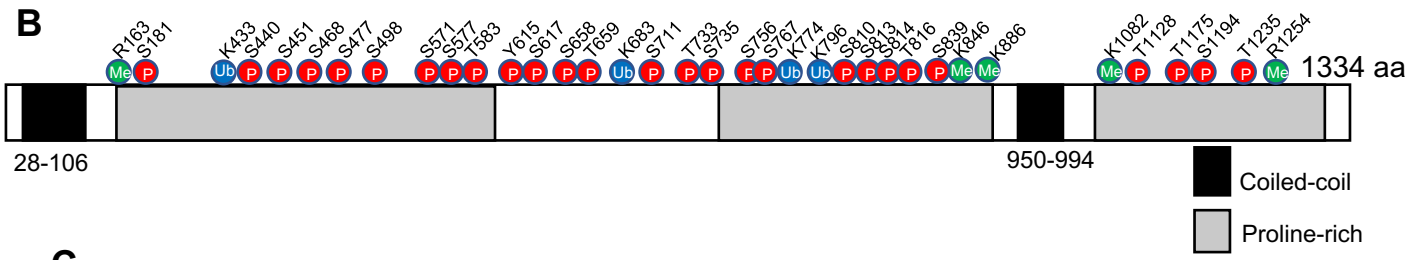


**C**

| Residue | Context | # PSM | Residue | Context | # PSM |
|---|---|---|---|---|---|
| S181 | ALDALsPFLRK | 6 | T733 | AVALGtNSLKQ | 4 |
| S440 | QIGPPsPGEAQ | 11 | S735 | ALGTNsLKQQE | 6 |
| S451 | GPLLPsPARGL | 3 | S756 | VYSSHsMGARV | 7 |
| S468 | PTSEKsPSPGG | 2 | S767 | DLEPVsPRSCL | 6 |
| S477 | GGPQLsPQLPR | 6 | S810 | GKPNKsPHSSP | 12 |
| S498 | SDGSPsPLLAR | 1 | S813 | NKSPHsSPTKL | 15 |
| S571 | TFRGPsPEPPP | 5 | S814 | KSPHSsPTKLP | 7 |
| S577 | PEPPPsPLQVP | 7 | T816 | PHSSPtKLPSK | 2 |
| T583 | PLQVPtYPQLE | 1 | S839 | LVTKEsPKPDK | 7 |
| Y615 | PESYPyGSPQE | 1 | T1128 | DSGIGtFPPPD | 1 |
| S617 | SYPYGsPQEKS | 1 | T1175 | PRRAHtLEREV | 3 |
| S658 | PGDPGsTPLRD | 3 | S1194 | SGRHPsMPAFP | 4 |
| T659 | GDPGStPLRDR | 3 | T1235 | LAKNWtFPNTR | 2 |
| S711 | GDMVPsIHRPL | 1 | | | |

**Figure 6. Post-translational modifications in Cep169 are identified by mass spectrometry.**
**(A)** Amino acid residues that undergo the following modifications are indicated (phosphorylation, red; methylation, green; ubiquitination, blue) in the primary structure of human Cep169 (GenBank accession number: NM_001037806.3).
**(B)** A schematic presentation of the structural motifs of Cep169, along with the modified residues.
**(C)** A list of Cep169 phosphorylated sites. The position of the phosphorylated residues and its context and number of detected PSMs (# PSM) are shown.

第 4 章については、５年以内に雑誌等で刊行予定のため、非公開。

第 4 章については、５年以内に雑誌等で刊行予定のため、非公開。

第 4 章については、５年以内に雑誌等で刊行予定のため、非公開。

第 4 章については、５年以内に雑誌等で刊行予定のため、非公開。

第 4 章については、５年以内に雑誌等で刊行予定のため、非公開。

第 4 章については、５年以内に雑誌等で刊行予定のため、非公開。

第 4 章については、５年以内に雑誌等で刊行予定のため、非公開。

第 4 章については、５年以内に雑誌等で刊行予定のため、非公開。

第 4 章については、５年以内に雑誌等で刊行予定のため、非公開。

第 4 章については、５年以内に雑誌等で刊行予定のため、非公開。

第 4 章については、５年以内に雑誌等で刊行予定のため、非公開。

第 4 章については、５年以内に雑誌等で刊行予定のため、非公開。

第 4 章については、５年以内に雑誌等で刊行予定のため、非公開。

第 4 章については、５年以内に雑誌等で刊行予定のため、非公開。

第 4 章については、５年以内に雑誌等で刊行予定のため、非公開。

第 4 章については、５年以内に雑誌等で刊行予定のため、非公開。

第 4 章については、５年以内に雑誌等で刊行予定のため、非公開。

第 4 章については、５年以内に雑誌等で刊行予定のため、非公開。

第 4 章については、５年以内に雑誌等で刊行予定のため、非公開。

第 4 章については、５年以内に雑誌等で刊行予定のため、非公開。

第 4 章については、５年以内に雑誌等で刊行予定のため、非公開。

第 4 章については、５年以内に雑誌等で刊行予定のため、非公開。

第 4 章については、５年以内に雑誌等で刊行予定のため、非公開。

第 4 章については、５年以内に雑誌等で刊行予定のため、非公開。

第 4 章については、５年以内に雑誌等で刊行予定のため、非公開。

第 4 章については、５年以内に雑誌等で刊行予定のため、非公開。

第 4 章については、５年以内に雑誌等で刊行予定のため、非公開。

第 4 章については、５年以内に雑誌等で刊行予定のため、非公開。

第 4 章については、５年以内に雑誌等で刊行予定のため、非公開。

第 4 章については、５年以内に雑誌等で刊行予定のため、非公開。

第 4 章については、５年以内に雑誌等で刊行予定のため、非公開。

第 4 章については、５年以内に雑誌等で刊行予定のため、非公開。

## 5. Conclusion

In this thesis, I have comprehensively studied the recently identified centrosomal protein Cep169 in human cells. First, hundreds of Cep169-interacting proteins and post-translational modifications of Cep169 *in vivo* have been successfully identified by proteomic analyses. These results strongly suggest that Cep169 participates in other unexpected cellular processes, including primary cilium formation. Second, functional cell biological assays have unveiled the novel function of Cep169 for the suppression of primary cilium formation in proliferating cells. In addition, these functional dissections provided unprecedented insights into the Cep169-mediated regulatory mechanisms of cilium formation.

## 6. Acknowledgements

The thesis study was performed under the supervision of Prof. Yasuhiko Terada (Waseda University, Japan). I would like to express my sincere gratitude for his keen mentorship and considerable support, which made it possible for this study to be accomplished.

Special thanks also go to Prof. Tetsuya Tabata (The University of Tokyo, Japan) for his support of this research.

I am also deeply grateful to Prof. Miho Ohsugi (The University of Tokyo, Japan) for her insightful comments and plentiful encouragement.

My sincere thanks also go to Prof. Yukiko Gotoh (The University of Tokyo, Japan), Dr. Maiko Higuchi (Rikkyo University, Japan), Dr. Tomohiko Okazaki (The University of Tokyo, Japan), and the members of the Gotoh laboratory, who provided an opportunity to join their team, and shared many valuable discussions about my research.

I would also like to thank the expert involved in the proteomic analysis, Dr. Lumi Negishi (The University of Tokyo). Without her accurate proteomic analysis, this research could not have been successfully conducted.

I am also grateful to another expert involved in primary cilium research, Dr. Tetsuo Kobayashi (Nara Institute of Science and Technology). Without his advice and valuable discussions, this research could not have been successfully conducted.

I am also grateful to the members of the Terada laboratory and the Tabata laboratory for many discussions and kind support.

Lastly, I would like to thank my family for all their love, support, and encouragement. Especially, I am most of all grateful for my loving, supportive, encouraging, and patient husband Keishi, whose faithful support is so heartening for me. Thank you.

## 7. References

Alves-Cruzeiro, J.M., Nogales-Cadenas, R., and Pascual-Montano, A.D. (2014). CentrosomeDB: a new generation of the centrosomal proteins database for Human and Drosophila melanogaster. Nucleic Acids Res *42*, D430-436.

Andersen, J.S., Wilkinson, C.J., Mayor, T., Mortensen, P., Nigg, E.A., and Mann, M. (2003). Proteomic characterization of the human centrosome by protein correlation profiling. Nature *426*, 570-574.

Barr, A.R., Kilmartin, J.V., and Gergely, F. (2010). CDK5RAP2 functions in centrosome to spindle pole attachment and DNA damage response. J Cell Biol *189*, 23-39.

Bettencourt-Dias, M., and Glover, D.M. (2007). Centrosome biogenesis and function: centrosomics brings new understanding. Nat Rev Mol Cell Biol *8*, 451-463.

Black, M.M., Slaughter, T., and Fischer, I. (1994). Microtubule-associated protein 1b (MAP1b) is concentrated in the distal region of growing axons. J Neurosci *14*, 857-870.

Cajanek, L., and Nigg, E.A. (2014). Cep164 triggers ciliogenesis by recruiting Tau tubulin kinase 2 to the mother centriole. Proc Natl Acad Sci U S A *111*, E2841-2850.

Choi, Y.K., Liu, P., Sze, S.K., Dai, C., and Qi, R.Z. (2010). CDK5RAP2 stimulates microtubule nucleation by the gamma-tubulin ring complex. J Cell Biol *191*, 1089-1095.

Conduit, P.T., Wainman, A., and Raff, J.W. (2015). Centrosome function and assembly in animal cells. Nat Rev Mol Cell Biol *16*, 611-624.

Dumont, J., and Desai, A. (2012). Acentrosomal spindle assembly and chromosome segregation during oocyte meiosis. Trends Cell Biol *22*, 241-249.

Fry, A.M., Leaper, M.J., and Bayliss, R. (2014). The primary cilium: guardian of organ development and homeostasis. Organogenesis *10*, 62-68.

Goetz, S.C., Liem, K.F., Jr., and Anderson, K.V. (2012). The spinocerebellar ataxia-associated gene Tau tubulin kinase 2 controls the initiation of ciliogenesis. Cell *151*, 847-858.

Heald, R., Tournebize, R., Habermann, A., Karsenti, E., and Hyman, A. (1997). Spindle assembly in Xenopus egg extracts: respective roles of centrosomes and microtubule self-organization. J Cell Biol *138*, 615-628.

Hilgendorf, K.I., Johnson, C.T., and Jackson, P.K. (2016). The primary cilium as a cellular receiver: organizing ciliary GPCR signaling. Curr Opin Cell Biol *39*, 84-92.

Honnappa, S., Gouveia, S.M., Weisbrich, A., Damberger, F.F., Bhavesh, N.S., Jawhari, H., Grigoriev, I., van Rijssel, F.J., Buey, R.M., Lawera, A.*, et al.* (2009). An EB1-binding motif acts as a microtubule tip localization signal. Cell *138*, 366-376.

Houlden, H., Johnson, J., Gardner-Thorpe, C., Lashley, T., Hernandez, D., Worth, P., Singleton, A.B., Hilton, D.A., Holton, J., Revesz, T.*, et al.* (2007). Mutations in TTBK2, encoding a kinase implicated in tau phosphorylation, segregate with spinocerebellar ataxia type 11. Nat Genet *39*, 1434-1436.

Hsu, P.D., Lander, E.S., and Zhang, F. (2014). Development and applications of CRISPR-Cas9 for genome engineering. Cell *157*, 1262-1278.

Inoko, A., Matsuyama, M., Goto, H., Ohmuro-Matsuyama, Y., Hayashi, Y., Enomoto, M., Ibi, M., Urano, T., Yonemura, S., Kiyono, T.*, et al.* (2012). Trichoplein and Aurora A block aberrant primary cilia assembly in proliferating cells. J Cell Biol *197*, 391-405.

Ishikawa, H., and Marshall, W.F. (2011). Ciliogenesis: building the cell's antenna. Nat Rev Mol Cell Biol *12*, 222-234.

Kim, S., Zaghloul, N.A., Bubenshchikova, E., Oh, E.C., Rankin, S., Katsanis, N., Obara, T., and Tsiokas, L. (2011). Nde1-mediated inhibition of ciliogenesis affects cell cycle re-entry. Nat Cell Biol *13*, 351-360.

Kobayashi, T., Kim, S., Lin, Y.C., Inoue, T., and Dynlacht, B.D. (2014). The CP110-interacting proteins Talpid3 and Cep290 play overlapping and distinct roles in cilia assembly. J Cell Biol *204*, 215-229.

Kobayashi, T., Tsang, W.Y., Li, J., Lane, W., and Dynlacht, B.D. (2011). Centriolar

kinesin Kif24 interacts with CP110 to remodel microtubules and regulate ciliogenesis. Cell *145*, 914-925.

Kurkowiak, M., Zietkiewicz, E., and Witt, M. (2015). Recent advances in primary ciliary dyskinesia genetics. J Med Genet *52*, 1-9.

Lechtreck, K.F. (2015). IFT-Cargo Interactions and Protein Transport in Cilia. Trends Biochem Sci *40*, 765-778.

Lu, Q., Insinna, C., Ott, C., Stauffer, J., Pintado, P.A., Rahajeng, J., Baxa, U., Walia, V., Cuenca, A., Hwang, Y.S.*, et al.* (2015). Early steps in primary cilium assembly require EHD1/EHD3-dependent ciliary vesicle formation. Nat Cell Biol *17*, 228-240.

Malumbres, M. (2014). Cyclin-dependent kinases. Genome Biol *15*, 122.

Masoud, K., Herzog, E., Chaboute, M.E., and Schmit, A.C. (2013). Microtubule nucleation and establishment of the mitotic spindle in vascular plant cells. Plant J *75*, 245-257.

Mori, Y., Inoue, Y., Tanaka, S., Doda, S., Yamanaka, S., Fukuchi, H., and Terada, Y. (2015a). Cep169, a Novel Microtubule Plus-End-Tracking Centrosomal Protein, Binds to CDK5RAP2 and Regulates Microtubule Stability. PLoS One *10*, e0140968.

Mori, Y., Inoue, Y., Taniyama, Y., Tanaka, S., and Terada, Y. (2015b). Phosphorylation

of the centrosomal protein, Cep169, by Cdk1 promotes its dissociation from centrosomes in mitosis. Biochem Biophys Res Commun *468*, 642-646.

Mori, Y., Taniyama, Y., Tanaka, S., Fukuchi, H., and Terada, Y. (2015c). Microtubule-bundling activity of the centrosomal protein, Cep169, and its binding to microtubules. Biochem Biophys Res Commun *467*, 754-759.

Nachury, M.V. (2014). How do cilia organize signalling cascades? Philos Trans R Soc Lond B Biol Sci *369*.

Nigg, E.A. (2007). Centrosome duplication: of rules and licenses. Trends Cell Biol *17*, 215-221.

Nigg, E.A., and Stearns, T. (2011). The centrosome cycle: Centriole biogenesis, duplication and inherent asymmetries. Nat Cell Biol *13*, 1154-1160.

Oda, T., Chiba, S., Nagai, T., and Mizuno, K. (2014). Binding to Cep164, but not EB1, is essential for centriolar localization of TTBK2 and its function in ciliogenesis. Genes Cells *19*, 927-940.

Paintrand, M., Moudjou, M., Delacroix, H., and Bornens, M. (1992). Centrosome organization and centriole architecture: their sensitivity to divalent cations. J Struct Biol *108*, 107-128.

Palazzo, R.E., Vogel, J.M., Schnackenberg, B.J., Hull, D.R., and Wu, X. (2000). Centrosome maturation. Curr Top Dev Biol *49*, 449-470.

Pazour, G.J., Dickert, B.L., Vucica, Y., Seeley, E.S., Rosenbaum, J.L., Witman, G.B., and Cole, D.G. (2000). Chlamydomonas IFT88 and its mouse homologue, polycystic kidney disease gene tg737, are required for assembly of cilia and flagella. J Cell Biol *151*, 709-718.

Pugacheva, E.N., Jablonski, S.A., Hartman, T.R., Henske, E.P., and Golemis, E.A. (2007). HEF1-dependent Aurora A activation induces disassembly of the primary cilium. Cell *129*, 1351-1363.

Rosenbaum, J.L., and Witman, G.B. (2002). Intraflagellar transport. Nat Rev Mol Cell Biol *3*, 813-825.

Sakaue-Sawano, A., Kurokawa, H., Morimura, T., Hanyu, A., Hama, H., Osawa, H., Kashiwagi, S., Fukami, K., Miyata, T., Miyoshi, H.*, et al.* (2008). Visualizing spatiotemporal dynamics of multicellular cell-cycle progression. Cell *132*, 487-498.

Sanchez, I., and Dynlacht, B.D. (2016). Cilium assembly and disassembly. Nat Cell Biol *18*, 711-717.

Satir, P., and Christensen, S.T. (2007). Overview of structure and function of mammalian cilia. Annu Rev Physiol *69*, 377-400.

Satir, P., Pedersen, L.B., and Christensen, S.T. (2010). The primary cilium at a glance. J Cell Sci *123*, 499-503.

Schmidt, K.N., Kuhns, S., Neuner, A., Hub, B., Zentgraf, H., and Pereira, G. (2012). Cep164 mediates vesicular docking to the mother centriole during early steps of ciliogenesis. J Cell Biol *199*, 1083-1101.

Schmidt, T.I., Kleylein-Sohn, J., Westendorf, J., Le Clech, M., Lavoie, S.B., Stierhof, Y.D., and Nigg, E.A. (2009). Control of centriole length by CPAP and CP110. Curr Biol *19*, 1005-1011.

Scholzen, T., and Gerdes, J. (2000). The Ki-67 protein: from the known and the unknown. J Cell Physiol *182*, 311-322.

Shaul, Y.D., and Seger, R. (2007). The MEK/ERK cascade: from signaling specificity to diverse functions. Biochim Biophys Acta *1773*, 1213-1226.

Shida, T., Cueva, J.G., Xu, Z., Goodman, M.B., and Nachury, M.V. (2010). The major alpha-tubulin K40 acetyltransferase alphaTAT1 promotes rapid ciliogenesis and efficient mechanosensation. Proc Natl Acad Sci U S A *107*, 21517-21522.

Singla, V., and Reiter, J.F. (2006). The primary cilium as the cell's antenna: signaling at a sensory organelle. Science *313*, 629-633.

Sluder, G. (2005). Two-way traffic: centrosomes and the cell cycle. Nat Rev Mol Cell Biol *6*, 743-748.

Spektor, A., Tsang, W.Y., Khoo, D., and Dynlacht, B.D. (2007). Cep97 and CP110 suppress a cilia assembly program. Cell *130*, 678-690.

Tang, C.J., Fu, R.H., Wu, K.S., Hsu, W.B., and Tang, T.K. (2009). CPAP is a cell-cycle regulated protein that controls centriole length. Nat Cell Biol *11*, 825-831.

Tanos, B.E., Yang, H.J., Soni, R., Wang, W.J., Macaluso, F.P., Asara, J.M., and Tsou, M.F. (2013). Centriole distal appendages promote membrane docking, leading to cilia initiation. Genes Dev *27*, 163-168.

Terada, Y., Uetake, Y., and Kuriyama, R. (2003). Interaction of Aurora-A and centrosomin at the microtubule-nucleating site in Drosophila and mammalian cells. J Cell Biol *162*, 757-763.

Tortosa, E., Galjart, N., Avila, J., and Sayas, C.L. (2013). MAP1B regulates microtubule dynamics by sequestering EB1/3 in the cytosol of developing neuronal cells. EMBO J *32*, 1293-1306.

Tucker, R.W., Pardee, A.B., and Fujiwara, K. (1979). Centriole ciliation is related to quiescence and DNA synthesis in 3T3 cells. Cell *17*, 527-535.

Wang, Z., Wu, T., Shi, L., Zhang, L., Zheng, W., Qu, J.Y., Niu, R., and Qi, R.Z. (2010). Conserved motif of CDK5RAP2 mediates its localization to centrosomes and the Golgi complex. J Biol Chem *285*, 22658-22665.

Westlake, C.J., Baye, L.M., Nachury, M.V., Wright, K.J., Ervin, K.E., Phu, L., Chalouni, C., Beck, J.S., Kirkpatrick, D.S., Slusarski, D.C.*, et al.* (2011). Primary cilia membrane assembly is initiated by Rab11 and transport protein particle II (TRAPPII) complex-dependent trafficking of Rabin8 to the centrosome. Proc Natl Acad Sci U S A *108*, 2759-2764.

Zheng, Y., Wong, M.L., Alberts, B., and Mitchison, T. (1995). Nucleation of microtubule assembly by a gamma-tubulin-containing ring complex. Nature *378*, 578-583.